The Journal of Experimental Biology 216, 1658-1669

doi:10.1242/jeb.079434

RESEARCH ARTICLE

The functional role of caudal and anal/dorsal fins during the C-start of a bluegill sunfish

Iman Borazjani

University at Buffalo, State University of New York, Buffalo, NY 14260, USA (iman@buffalo.edu)

SUMMARY

Fast starts are crucial in the survival of aquatic swimmers to capture prey or avoid predators. Currently, it is widely accepted that during C-starts: (1) the caudal fin generates a considerable hydrodynamic force; and (2) anal/dorsal fins are erected to significantly increase the hydrodynamic force. In this work, the above hypotheses on the role of fins during C-starts are studied using experimentally guided numerical simulations of four bluegill sunfish, whose fins are removed or erected. The amount of force created by the body and fins at each time instant was not constant and varied during the C-start. Nevertheless, in agreement with hypothesis (1), up to 70% of the instantaneous hydrodynamic force was generated by the tail during Stage 2 of the C-start, when the sunfish rapidly bends out of the C-shape. Additionally, the contribution in Stage 1, when the sunfish bends into a C-shape, is less than 20% at each instant. Most of the force in Stage 1 was produced by the body of the sunfish. In contrast to hypothesis (2), the effect of erection/removal of the fins was less than 5% of the instantaneous force in both Stages 1 and 2, except for a short period of time (2 ms) just before Stage 2. However, it is known that the anal/dorsal fins are actively controlled during the C-start from muscle activity measurements. Based on the results presented here, it is suggested that the active control of the anal/dorsal fins can be related to retaining the stability of the sunfish against roll and pitch movements during the C-start. Furthermore, the erection of the fins increases the moment of inertia to make the roll and pitch movements more difficult.

Supplementary material available online at http://jeb.biologists.org/cgi/content/full/216/9/1658/DC1

Key words: C-start, rapid start, escape, fin, numerical simulation, bluegill sunfish, hydrodynamics.

Received 11 September 2012; Accepted 2 January 2013

INTRODUCTION

The kinematics (body motion) during fast starts of fish is quite different from steady swimming. During the C-start, the sunfish bends its body into a C-shape, which is followed by one or more alternating tail beats (Domenici and Blake, 1997; Tytell and Lauder, 2008). The C-start behavior has been divided into two major phases: Stage 1, the initial C-bend; and Stage 2, the stroke in which the body bends out of the C-shape (Weihs, 1973). Fast-start maneuvers have significant fitness consequences for aquatic animals as they are used to flee predators (Walker et al., 2005) or to capture prey (Webb, 1984; Harper and Blake, 1991; Canfield and Rose, 1993). Such fitness consequences have probably created a strong selective pressure in the evolution of fish. Therefore, the C-start has been extensively studied in terms of muscle activity (Jayne and Lauder, 1993; Wakeling and Johnston, 1998; Westneat et al., 1998; Wakeling and Johnston, 1999; Wakeling et al., 1999; Ellerby and Altringham, 2001; Tytell and Lauder, 2002), neural control (Fetcho, 1991; Zottoli et al., 1995; Eaton et al., 2001; Tytell and Lauder, 2002; Koyama et al., 2011), and kinematics (Domenici and Blake, 1991; Domenici and Blake, 1993; Spierts and Leeuwen, 1999); see also the review by Domenici and Blake (Domenici and Blake, 1997).

To understand the evolution of body and fin morphology in a fish species, one must examine how body/fin shape and kinematics affect the underlying mechanisms of hydrodynamic force and power generation (Blake, 2004). The objective of this work was to investigate the effect of fins during the C-start. The conventional wisdom is that the fins contribute significantly to the hydrodynamic force generated during the C-start (Webb, 1977; Frith and Blake, 1991; Tytell and Lauder, 2008; Chadwell et al., 2012a; Chadwell et al., 2012b). The results presented here agree with the conventional wisdom for the caudal fin, but challenge it for the anal/dorsal fins.

Early studies have extended Lighthill's (Lighthill, 1971) elongated body theory (EBT) to approximate the forces during turning and fast starts (Weihs, 1972; Weihs, 1973). According to EBT, developed by Weihs (Weihs, 1972; Weihs, 1973) for fast starts and turning maneuvers, two types of forces are generated by the body motion: forces by accelerating the adjacent fluid, i.e. non-circulatory reacting (added mass) force, and lift forces contributing to thrust by fins. Note that EBT (Lighthill, 1971) is an inviscid theory in which forces are generated only due to the motion perpendicular to the fish spinal column by the added mass effect (Weihs, 1972). The body motion tangent to the fish spinal column does not affect the forces due to the slip of inviscid fluid over the fish body. Furthermore, according to EBT, a larger body and fin area perpendicular to the fish spinal column (larger depth along the spinal column) is advantageous for fast starts because a larger amount of water can be accelerated by the body, i.e. higher added mass force (Weihs, 1972; Weihs, 1973).

The pioneering work of Webb (Webb, 1977) investigated the effect of fins on the C-start performance by measuring the average acceleration of fish. He amputated the fin rays of rainbow trout in eight different ways (Webb, 1977): control (pelvic rays amputated); dorsal fin; anal fin; dorsal lobe of caudal fin and ventral lobe of caudal fin; ventral lobe of caudal fin and anal fin; dorsal and ventral lobes of caudal fin; and both caudal-fin lobes and anal fin. The series represents progressive reduction in fin and body area, as well as

reduction in the areas where lateral movements are largest (Webb, 1977), whose acceleration should decrease according to the EBT. However, the change in mean acceleration of the fish was statistically insignificant for the first six groups (<5%) relative to the control. Only the last three groups, for which the caudal fin lobes were removed, showed a statistically significant decrease in the mean acceleration (Webb, 1977), i.e. his results were inconclusive on the effect of anal/dorsal fins on the hydrodynamic forces. The results presented here will provide an explanation for these results.

In another investigation, Webb (Webb, 1978) compared fast-start performance of seven different species of fish in terms of maximum and mean acceleration rate. He found that the fast-start performance depended primarily on compromise between muscle mass, as a percentage of body mass, and lateral body and fin profile. He argued based on EBT that the large body depth at locations with high lateral velocity are important for better performance. However, enough muscle mass and depth should be retained near the center of mass to minimize recoil (lateral motion of the center of mass). In Webb's study the function of the anal/dorsal and the caudal fin was not the focus, and the performance of the different species was compared (Webb, 1978). Many other studies have focused on C-start performance of individual fish species and have provided valuable information on the acceleration of fish center of mass and its kinematics (e.g. Webb and Skadsen, 1980; Webb, 1984; Harper and Blake, 1988; Domenici and Blake, 1991; Harper and Blake, 1991; Domenici and Blake, 1993; Webb et al., 1996; Domenici and Batty, 1997; Bergstrom, 2002; Domenici et al., 2004). The digitization and numerical differentiation error of such measurements has been discussed previously (Harper and Blake, 1989; Walker, 1998). The role of fins was not conclusively elucidated in the above studies.

Several researchers have studied the hydrodynamics of the turning maneuver (Wolfgang et al., 1999; Epps and Techet, 2007; Müller et al., 2008), whereas the fast start was first studied by Tytell and Lauder (Tytell and Lauder, 2008). The hydrodynamics and kinematics of the turning maneuver is similar to fast start, albeit slower. However, the neural control in these two behaviors is quite different. More recently a mechanical fish has been used to study the hydrodynamics of the C-start (Conte et al., 2010; DeVoria and Ringuette, 2012). In such experimental studies, the flow has been typically measured using particle image velocimetry (PIV) and the hydrodynamic force is approximated based on the measured flow field. Tytell and Lauder (Tytell and Lauder, 2008) estimated that dorsal and anal fins contribute 37% of total momentum. However, they cautioned that the body near the fins can contribute to the flow momentum measured in the planes passing through the dorsal and anal fins. Frith and Blake, using Weihs's EBT, estimated that more than 90% of the positive total thrust during the propulsive stage is created by the caudal area, ~77% is generated by the caudal fin, and 28% by the anal and dorsal fins in the pike *Esox lucius* (Frith and Blake, 1991).

Borazjani et al. (Borazjani et al., 2012) studied the C-start of a bluegill sunfish using numerical simulations based on the experimentally measured kinematics (Tytell and Lauder, 2008). Their simulations were in great agreement with the PIV measurements and could capture all the flow features (Tytell and Lauder, 2008). Furthermore, for the first time, their simulations showed: (1) the 3-D wake structure during the C-start consisting of multiple vortex rings; (2) the effect of Reynolds number; and (3) the importance of calculating forces based on the 3-D flow field. Nevertheless, the role of the fins on the force generation at different time instants during the C-start was not studied by Borazjani et al. (Borazjani et al., 2012). Recently, Gazzola et al. (Gazzola et al., 2012) studied the C-start of larval fish using simulations with an evolutionary optimization for the kinematics. They found that the best motions to maximize the distance travelled are similar to the experimentally observed C-start maneuvers. The focus of this paper is not on optimizing the kinematics, but on the role of fins during the C-start.

It has been observed that the anal and dorsal fins are controlled actively by the muscles (Jayne et al., 1996; Standen and Lauder, 2005; Lauder et al., 2007; Chadwell and Ashley-Ross, 2012; Chadwell et al., 2012a; Chadwell et al., 2012b). During the C-start, these fins are rapidly erected to increase their surface area (Webb, 1977; Jayne et al., 1996; Tytell and Lauder, 2008; Chadwell and Ashley-Ross, 2012). Based on EBT and recent flow momentum measurements, it has been hypothesized that these fins play an important role in generating hydrodynamic force for the C-start. The results presented here contradict this view by showing that the contribution of anal and dorsal fin to the hydrodynamic force is minimal. Here an alternative hypothesis for the role of these fins is provided, which states that the role of these fins is to increase stability similar to the long stick held by rope walkers. The objective of this work is to quantitatively demonstrate the effects of fins (caudal and anal/dorsal) on the C-start. This is achieved by creating different virtual sunfish with the fins removed/erected and comparing them with respect to the forces and the 3-D flow field they create.

MATERIALS AND METHODS

The virtual swimmer's geometry (Fig. 1A) is generated from a computed tomography (CT) scan of a bluegill sunfish (provided by G. V. Lauder, Harvard University). Three other swimmers are constructed by removing the anal/dorsal fins (Fig. 1C), removing the caudal fin (Fig. 1D), and erecting the anal/dorsal fins (Fig. 1E). The anal/dorsal fin area removed is about $0.025L^2$, where L is the length of the control sunfish (Fig. 1C). For the erected fins, the area is increased threefold, which is similar to the experimental measurements of the maximum fin area of a typical bluegill sunfish (Chadwell et al., 2012a; Chadwell et al., 2012b). Furthermore, this is consistent with Webb's measurements that the anal fin depth was increased by about 1 cm and the dorsal fin by about 0.25 cm for a rainbow trout (Webb, 1977). The fish geometries are meshed using a triangular grid as required by the numerical method. The C-start kinematics for all of the swimmers are reconstructed using the same method based on experimental measurements (Tytell and Lauder, 2008) by cubic spline interpolation implemented in CMATH libraries (Jacobs and Lott, 1989), in both time and space (Borazjani et al., 2012). Fig. 1F shows the C-start kinematics for the mid-line of the fish from experimental measurements (Tytell and Lauder, 2008). By comparing the forces and the flow field created by the swimmers with the fins removed/erected (Fig. 1C–E) against the control (Fig. 1A), the effect of caudal fin and dorsal/anal fins during the C-start will be investigated.

The sharp-interface immersed boundary method (Gilmanov and Sotiropoulos, 2005) is used to solve the incompressible, unsteady, three-dimensional Navier–Stokes equations over the grid in which the fish body is immersed. The immersed boundary method has been described in detail in previous publications (Gilmanov and Sotiropoulos, 2005; Ge and Sotiropoulos, 2007; Borazjani et al., 2008) and only a brief description of the technique is given here. An unstructured, triangular mesh is used to discretize and track the position of the fish body. Boundary conditions for the velocity field at the Cartesian grid nodes that are exterior to but in the immediate vicinity of the immersed boundary (IB) nodes are reconstructed by quadratic interpolation along the local normal to the boundary. The

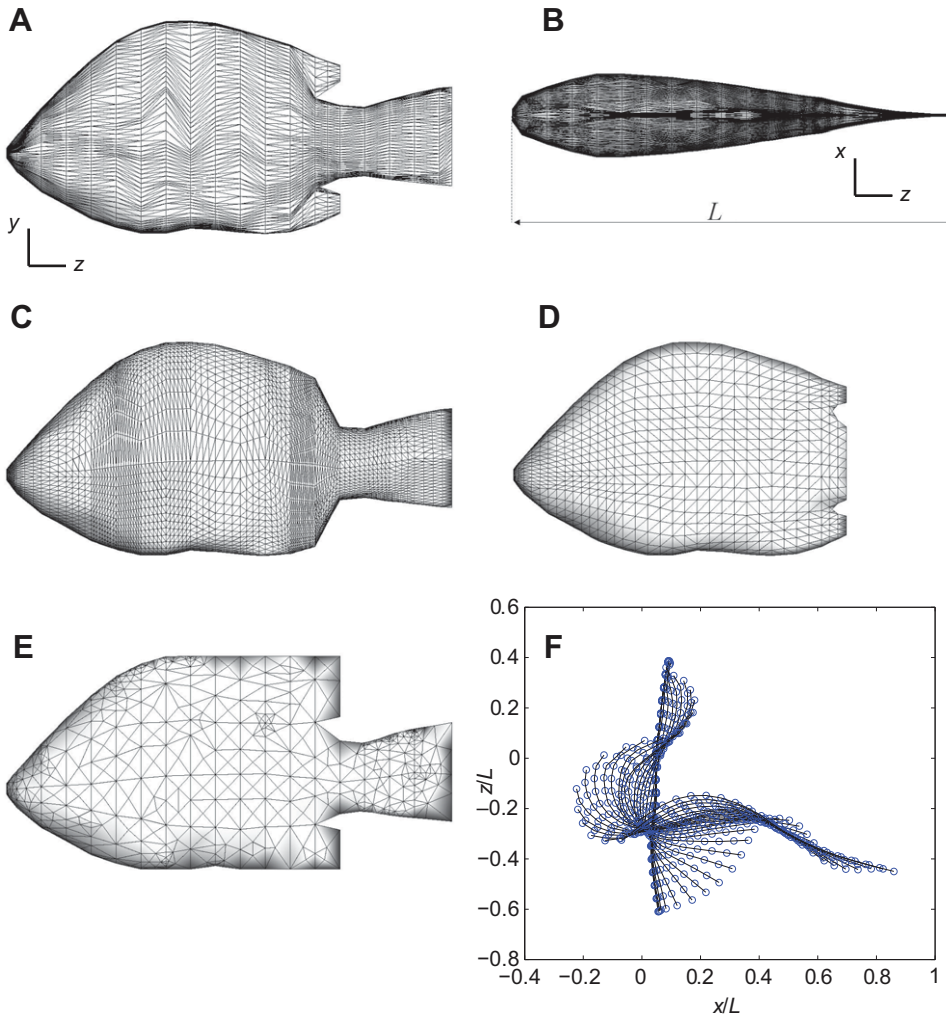

Fig. 1. The geometry of the bluegill sunfish (A) reconstructred from the CT scan images from top view and (B) side view. Three other virtual swimmers are reconstructed by removing (C) anal and dorsal fins and (D) the caudal fin (tail), and (E) erecting the anal and dorsal fins. All virtual swimmers are meshed with triangular elements as required by the immersed boundary method. (F) The mid-lines of the fish at several time instants during the C-start from experimental measurements (Tytell and Lauder, 2008). The fish length L is 10.71 cm.

reconstruction method has been shown to be second-order accurate (Gilmanov and Sotiropoulos, 2005; Borazjani et al., 2008). The IB nodes at each time step are recognized using an efficient ray-tracing algorithm (Borazjani et al., 2008). As in previous studies (Borazjani and Sotiropoulos, 2008; Borazjani and Sotiropoulos, 2009; Borazjani and Sotiropoulos, 2010; Borazjani et al., 2012), an efficient fractional step method is used to advance the flow solution in time (Ge and Sotiropoulos, 2007). The Poisson equation is solved with FGMRES (Saad, 2003) and multigrid as a preconditioner using parallel libraries of PETSc (Balay et al., 2001).

The method has been validated extensively for other flows with moving boundaries (Gilmanov and Sotiropoulos, 2005; Borazjani et al., 2008) and has also been applied to simulate steady swimming of tethered (Borazjani and Sotiropoulos, 2008; Borazjani and Sotiropoulos, 2009) and self-propelled (Borazjani and Sotiropoulos, 2010) carangiform and anguilliform swimmers, as well as the wake structure of anatomically realistic copepods (Borazjani et al., 2010). Furthermore, it has been applied to simulate the C-start of a bluegill sunfish (Borazjani et al., 2012), and the simulated flow field could capture all the flow features observed in experiments and was in excellent agreement with the PIV measurements (Tytell and Lauder, 2008).

The computational domain within which the fish body is immersed extends $40L\times4L\times40L$, where L is the body length of the fish, in the x-, y- and z-directions, respectively (see Fig. 1 for definition of the coordinates). Note that the vertical extent $4L$ of the domain is eight times the bluegill sunfish depth of $0.5L$ in the y-direction. This domain is discretized with a Cartesian grid with $201\times101\times201\approx4$ million grid points. A uniform, fine mesh with spacing $0.01L$ is used inside an inner region ($L\times0.5L\times L$) that contains the fish body during the C-start. Outside this inner box the grid is stretched to the outer boundaries of the domain using the hyperbolic tangent function. The time step for the simulations Δt^* is set equal to 1/8 of the time step Δt_{exp} used to collect PIV data in the experiments, i.e. $\Delta t^*=\Delta t_{exp}/8=0.125$ ms. A non-dimensional time step $\Delta t=U\Delta t^*/L=0.003$ is used in the simulations to ensure the stability and that the fish body motion at each time step is restricted to only one grid point. This choice of a non-dimensional time step results in a velocity scale of $U=2.57\,m\,s^{-1}$ considering the fish length $L=10.71$ cm. All the other variables are non-dimensionalized using the fish body length as length scale $L=10.71$ cm and the velocity scale $U=2.57\,m\,s^{-1}$, which is about 80% of the maximum fish body velocity. These computational details are exactly the same as in previous work (Borazjani et al., 2012). The durations of Stages 1 and 2 are 32 and 25 ms, respectively, i.e. the complete C-start lasts about 57 ms. The Reynolds number (Re) is defined as:

$$Re = UL/\upsilon, \quad (1)$$

where υ is the kinematic viscosity of the fluid, U is the velocity scale and L is the fish length. For water as a working fluid, the Reynolds number of the experiments is about 275,000. This Reynolds number is well within the inertial regime, in which inertial

forces dominate the viscous forces and determine the flow physics. Therefore, given the fact that the viscous forces are not expected to influence the dynamics of the flow in this regime, and since viscous flow simulations fully resolving the boundary layer on the body of the fish are impractical at such high Reynolds number, inviscid (Re=∞) simulations are performed similar to previous work (Borazjani et al., 2012). Furthermore, viscous simulations at Re=4000 are carried out to investigate the effect of the Reynolds number similar to previous work (Borazjani et al., 2012). In an experiment with live fish, reducing the Reynolds number is equivalent to either a smaller-size fish performing a similarly fast C-start, or using the same fish performing a slower turn. The same method for both Re=4000 and Re=∞ simulations is used. The difference between these simulations is how the velocity on the immersed boundary nodes, adjacent to the fish body, is reconstructed. At Re=4000, the velocity at the immersed boundary nodes is reconstructed based on no-slip boundary conditions on the fish body, i.e. fluid velocity on the fish body is equal to the velocity of the fish body. However, at Re=∞ the velocity at the immersed boundary nodes is reconstructed based on slip-wall boundary conditions at the fish body, i.e. the flow velocity in the normal direction is equal to the normal velocity of the fish body (no-flux), whereas the tangential flow velocity is independent of the tangential velocity of the fish body and is extrapolated from the inner fluid nodes (slip).

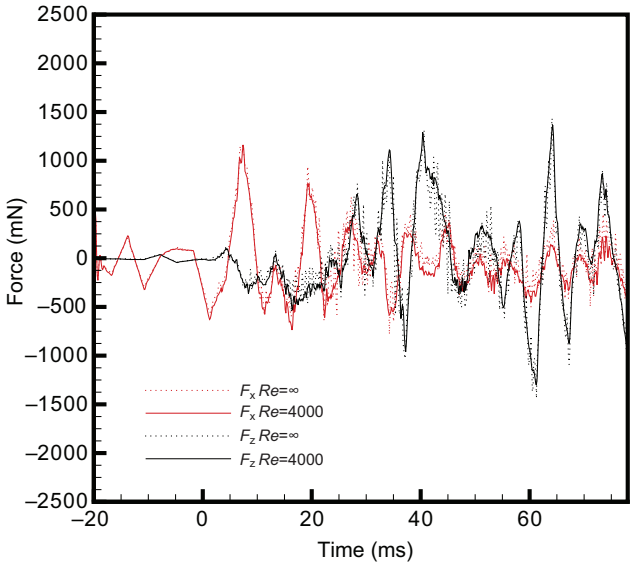

Fig. 2. Sunfish with no caudal fin simulations: comparison of the force history between Re=4000 and Re=∞ simulations during the C-start. The Re=∞ time history shows high-frequency oscillations around the Re=4000 results. Nevertheless, both time histories show similar trends.

RESULTS

In this section the hydrodynamic forces created during the C-start by the swimmers with different fins are compared. The pressure on the surface of the fish is also examined to identify the regions of high and low pressure that contribute most to the force. The wake structure and pressure fields are then examined to identify the reasons for the observed differences as the hydrodynamic forces are the direct consequence of a transfer of momentum from the fish body and fins to the water.

Hydrodynamic forces

The difference in fins of the virtual swimmers results in the difference in the momentum transferred to the fluid, i.e. different hydrodynamic forces during the C-start. Fig. 2 shows the forces during a complete C-start exerted by the fluid on the sunfish with no caudal fin in the x- and z-directions. As demonstrated in Fig. 2, similar to previous work (Borazjani et al., 2012), both the Re=∞ and Re=4000 simulations exhibit the same overall trends, with the former yielding a somewhat more spiky distribution and larger magnitude extrema than the latter. This is consistent with the fact that at low Re, viscous stresses have stronger dissipative effects, i.e. dissipate and smooth out the hydrodynamic forces. Nevertheless, similar trends in Re=∞ and Re=4000 simulations show that the inertial forces dominate the viscous forces during the C-start. The spiky distribution of Re=∞ force around Re=4000 force history (Fig. 2) should not be confused with the large-amplitude fluctuations occurring over a time scale of the order of few milliseconds in both Re=∞ and Re=4000 force history (Borazjani et al., 2012). These force fluctuations are larger in the x-component of the force during Stage 1, whereas they are far more pronounced in the z-component of the force during Stage 2 (Fig. 2). This trend is obviously related to rapidly changing orientation of the fish body, which is mainly oriented in the z-direction during Stage 1 and the x-direction during Stage 2, and the fact that the primary force component during each stage is in the lateral direction to the body (Borazjani et al., 2012). These large fluctuations are related to the change in the direction of the acceleration of the fish mid-line, which changes the location of the high and low pressure pockets around the fish; see previous work for more details (Borazjani et al., 2012). Force fluctuations during the C-start have also been observed in previous numerical and experimental work (Harper and Blake, 1989; Harper and Blake, 1991; Wolfgang et al., 1999).

The force history of all other swimmers, although not shown here, at both Re=∞ and Re=4000 show similar trends, with Re=4000 force being smoother. Therefore, to compare different swimmers, the force histories at Re=4000 are chosen, which are smoother and make the differences in forces created by the four sunfish easier to discern. Fig. 3 shows the force history of all swimmers at Re=4000 during the C-start. First, the effect of anal/dorsal fins during the C-start is investigated by comparing the forces between the sunfish with all fins (control sunfish) and the sunfish with anal/dorsal fins removed and erected. It can be observed in Fig. 3 that the discrepancy between the forces created by the control sunfish and the sunfish with anal/dorsal fins removed and erected is quite small. The largest difference in forces occurs at local minima and maxima of the force history. However, they are still within 1% of each other. At all other instants the forces are almost identical. The only exception is at the end of Stage 1. At around t=30 ms to 32 ms, the difference between the erected fins and control is relatively large (about 70 mN). In the same time frame the difference between the no-tail and control is about 400 mN. This indicates that the removal or erection of the dorsal and anal fins does not contribute much to the total hydrodynamic forces, except for a short period of time (~2 ms) just before Stage 2 (Fig. 3).

To investigate the effect of the caudal fin, the forces created by the sunfish with no tail were compared against the sunfish with all the fins (control sunfish). It was observed that the sunfish with no tail showed greater difference than the sunfish with fins removed/erected relative to the control sunfish (Fig. 3), i.e. the caudal fin contributes more to the total hydrodynamic force than the anal/dorsal fins. It should be noted that the difference between forces created by the sunfish with no tail and the control is not constant

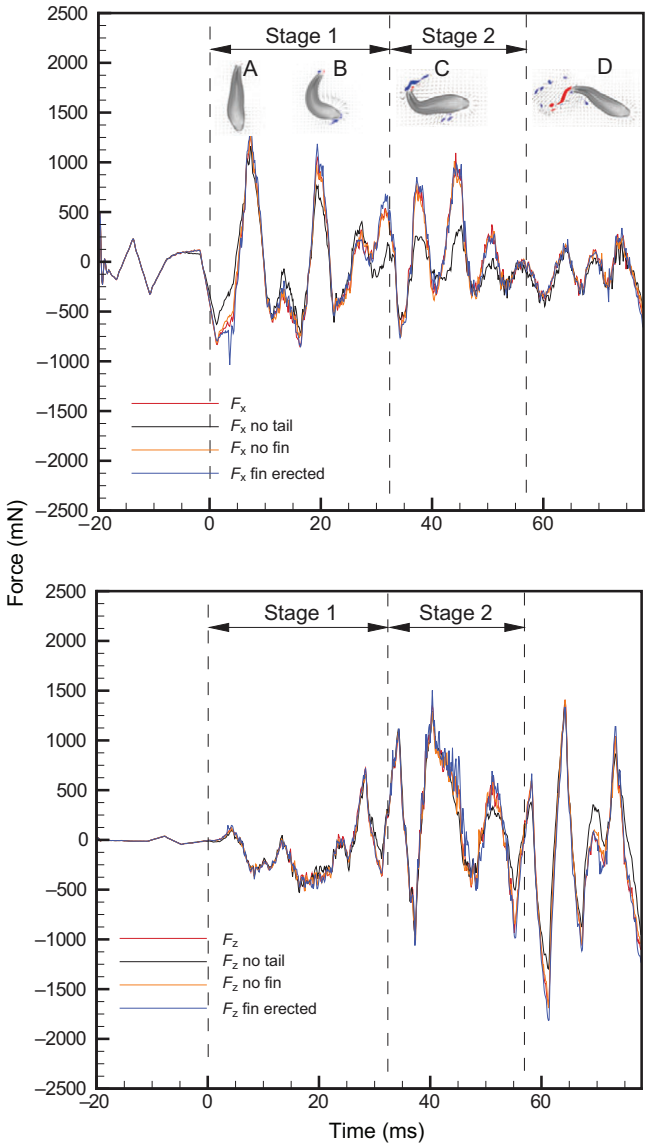

Fig. 3. The force history from *Re*=4000 simulations during the C-start in the *x* (top) and *z* (bottom) directions for the four different sunfish. The insets show the body shape of the sunfish with no tail at *t* of 5 ms (A), 21 ms (B), 41 ms (C) and 71 ms (D).

and varies in time, depending on the orientation and motion of the tail. During Stage 1, the sunfish (originally oriented mainly in the *z*-direction) starts to make the C-shape by moving the tail and the head in the *x*-direction. Because the motion of the tail is mainly in the *x*-direction in this stage (see inset B in Fig. 3), the removal of the tail mainly affects the *x*-component of the force. The removal of the tail does not affect the *z*-component (F_z) until the end of Stage 1 (t=30 ms), when the tail has finished the motion in the *x*-direction and turns to face the *z*-direction.

At the beginning of Stage 2, the tail bends out of the C-shape by moving primarily in the negative *x*-direction (Fig. 3C). Therefore, as can be observed from Fig. 3, removing the tail mainly affects the *x*-component of the force (F_x) early in Stage 2. In fact, the largest difference between the forces, caused by removing the tail, is observed in Stage 2 at the time instant about 30 to 55 ms in the F_x, e.g. at t=44 ms the difference in F_x is about 700 mN. Furthermore, because the tail motion, and consequently the flow momentum, is mainly in the *x*-direction during early Stage 2, as observed in Fig. 3, F_z is relatively unaffected by removing the tail. At the end of Stage 2 (t>50 ms) F_z shows greater difference because the sunfish is out of the C-shape and oriented in the *x*-direction, i.e. the body and tail move laterally in the *z*-direction (Fig. 3D). The difference in F_z is about 200 mN during the end of Stage 2.

Wake structure

The difference in hydrodynamic forces (Fig. 3) is the result of different transfers of momentum from the virtual swimmers to the water. Different transfers of momentum result in different vortical structures in the wake of the swimmers. Therefore, the wake structure was investigated to identify the reasons for the observed differences in the hydrodynamic forces. The wake structure is analyzed in terms of the flow field in the mid-plane of the swimmers as well as the 3-D vortical structures, and the relation with the hydrodynamic force is discussed in what follows.

The flow field in the mid-plane of the swimmers was visualized using velocity vectors and vorticity contours in Fig. 4. Three fluid jets have been identified during the C-start of the sunfish with all the fins (control) in previous experiments (Tytell and Lauder, 2008), and their simulations (Borazjani et al., 2012). Also, three fluid jets are identified in Fig. 4 for all virtual sunfish whose tails are intact. These jets are the result of a transfer of momentum from the fish body and fins during the escape response. Jet 1 is formed by the tail during the initial C-bend in Stage 1 (Fig. 4B), and is fully developed during Stage 2 (Fig. 4C,D). Therefore, it is visible in the flow field of all sunfish whose tails are intact, but not in the flow field of the sunfish whose tail is removed. Jet 2 is created by the middle of the body during the initial C-bend in Stage 1 (Fig. 4B), and the tail adds momentum to it during Stage 2 as the fish bends out of the C-shape and turns after Stage 1 (Fig. 4C,D). Jet 2 is fully developed at the end of Stage 2. During Stage 1, the direction of Jet 2 for all sunfish is almost the same in the negative *x*-direction. However, in Stage 2 all sunfish with tails intact have the Jet 2 flow in the negative *x*-direction, but the tail-less sunfish has the Jet 2 flow in a 45 deg angle relative to the *x*-direction. In fact, the removal of the tail does not affect the Jet 2 flow (but affects Jet 1) in Stage 1, but affects both Jet 1 and Jet 2 in Stage 2. The change in the direction of Jet 2 reduces the momentum in the *x*-direction, causing a much lower force in the *x*-direction during Stage 2 (Fig. 3). Finally, Jet 3 is formed near the middle of the body but on the opposite side of Jet 2, during Stage 2 and later (Fig. 4C,D). This jet formed an approximate 45 deg angle with the *x*-direction in the flow of all sunfish. Since this jet is mainly created by the mid-body section, the removal of tails did not seem to affect it (Fig. 4C,D). In the tail-less sunfish, this jet (Jet 3) is almost parallel, but in the opposite direction to Jet 2 (Fig. 4D), i.e. the momentum of Jet 2 is almost cancelled out with momentum of Jet 3, creating much less hydrodynamic force during Stage 2, in agreement with previous hydrodynamic force plots (Fig. 3).

Besides the velocity vectors and fluid jets, the development of vorticity can also be observed in Fig. 4. The motion of the tail to create the initial C-bend creates a positive vorticity at the end of the tail, just above Jet 1 (VT1 in Fig. 4B). To get out of the C-bend, the motion of the tail in the opposite direction during Stage 2 creates negative vorticity at the end of the tail, just below Jet 1 and the previous positive vorticity (VT2 in Fig. 4C). Therefore, Jet 1 flows through two, well-defined counter-rotating vortices (VT1 and VT2 in Fig. 4C,D). The two counter-rotating vortices are observed in all of the sunfish except the sunfish with no tail. This is due to the fact that these vortices are created by the motion of the tail, which do not exist in the tail-less sunfish. Jet 2 has less clearly defined vortices. Instead, as the tail

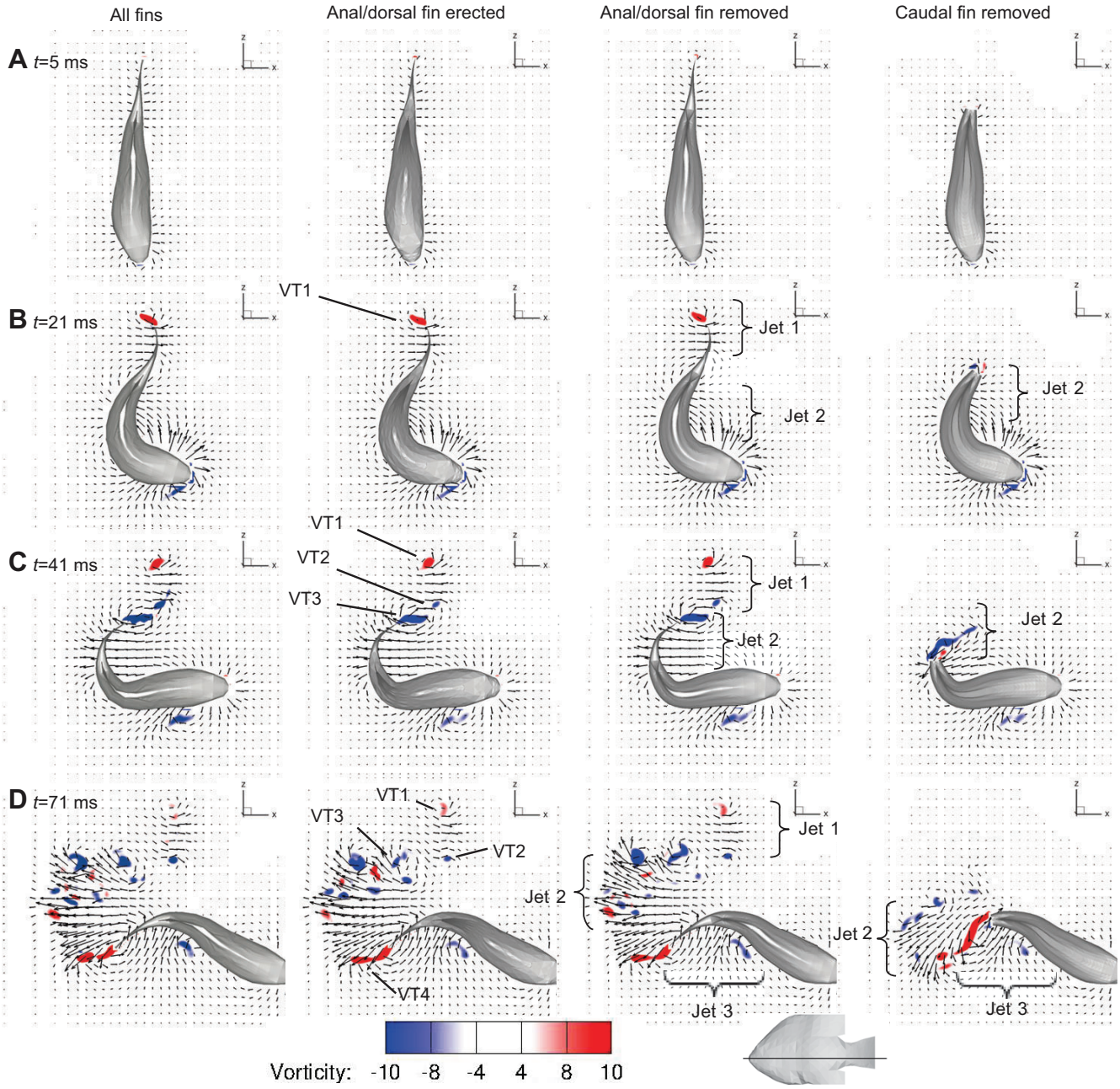

Fig. 4. The flow in the mid-plane of the sunfish visualized by velocity vectors and contours of non-dimensional vorticity at *t* of 5 ms (A), 21 ms (B), 41 ms (C) and 71 ms (D) for the sunfish with no side fins (left column) and the swimmer with no tail (right column). The three dominant jet flows are labelled. Peak flow velocities are nearly 1 m s^{-1}. The black line on the bluegill icon at the bottom indicates the location of the mid-plane in this sequence. In this escape, Stage 1 lasted for 32 ms and Stage 2 for 25 ms; therefore the whole escape lasted 57 ms. The vortices created by the tail are denoted by VT1 to VT4. Only every fourth vector is shown for clarity.

moves to get out of the C-bend during Stage 2, it creates a strong shear layer (VT3 Fig. 4C) that becomes unstable and breaks into smaller vortices (VT3 in Fig. 4D). In all of the sunfish with tails intact, this shear layer is in the *x*-direction and created by the tail, but in the tail-less sunfish it is almost at a 45 deg angle created by the end of the body (VT3 in Fig. 4C). This shear layer for all sunfish breaks into smaller vortices (VT3 in Fig. 4D), and a new shear layer (VT4 with positive vorticity) is created by the motion of the tail or the end of the body in the opposite direction. Jet 3 was accompanied by a small amount of vorticity near the head during Stage 1 (Fig. 4B), which became more diffused during Stage 2 (Fig. 4C,D).

The differences in the vorticity in the 2-D plane correspond to differences in the 3-D wake. Here the linkage between the 3-D structure of the wake and the various jets identified above, and the hydrodynamic force is investigated. The 3-D wake structure is visualized in Fig. 5 using iso-surfaces of the *q*-criteria (Hunt et al., 1988) at the same time instants as Fig. 4 for all of the sunfish for $Re=\infty$ simulations; see supplementary material Movies 1–3 for videos of evolution of the wake structure at $Re=4000$. According to Hunt et al., regions where $q>0$, i.e. regions where the rotation rate dominates the strain rate, are occupied by vortical structures (Hunt et al., 1988).

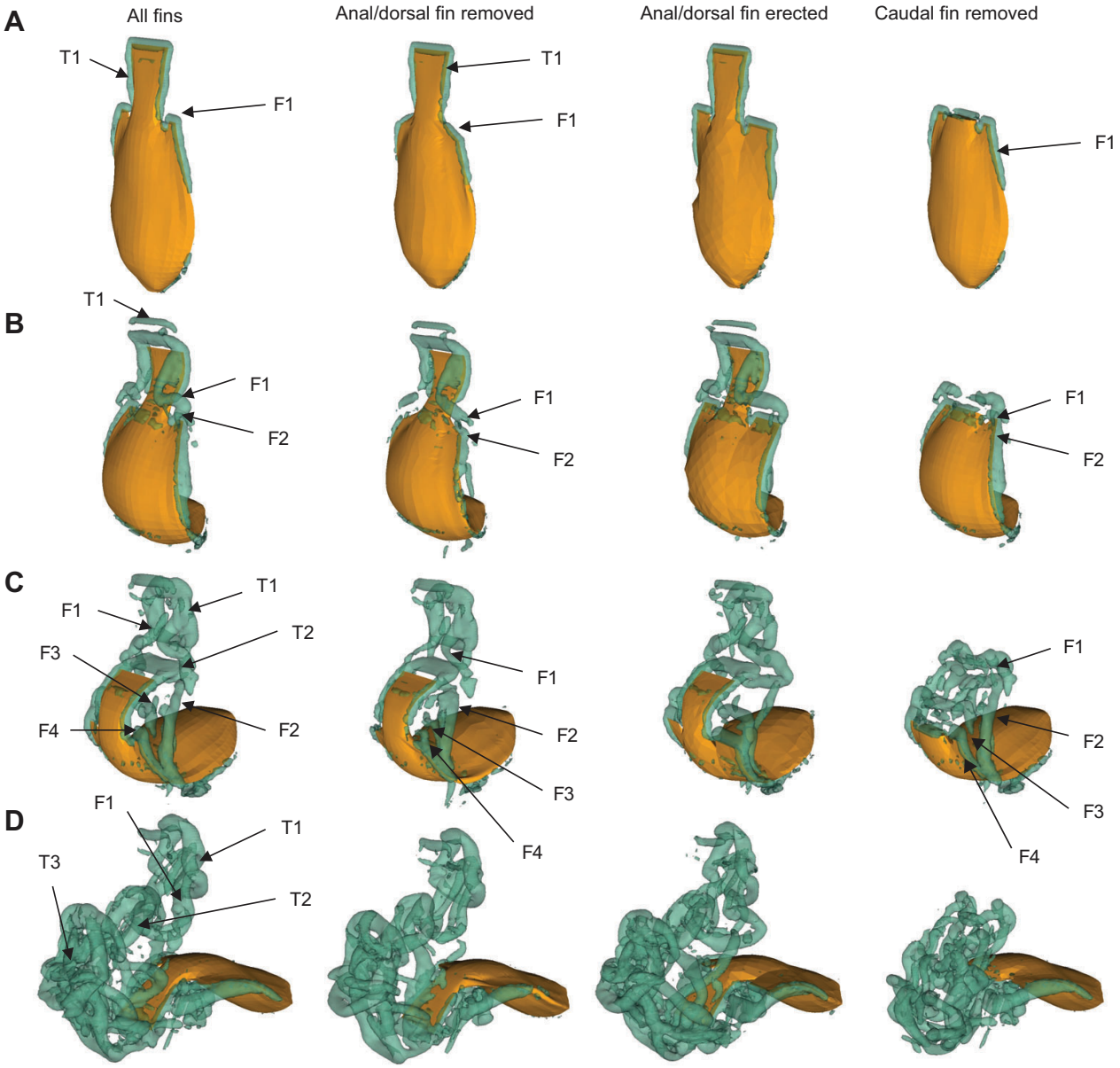

Fig. 5. Three-dimensional vortical structure visualized by the iso-surfaces of *q*-criterion for the sunfish with all fins, no anal/dorsal fins, anal/dorsal fins erected, and no tail at *t* of 5 ms (A), 21 ms (B), 41 ms (C) and 71 ms (D). The vortical structures created by the tail are marked T1 to T3 and the ones created by the anal/dorsal fins are marked F1 to F4. See supplementary material Movies 1–3 for videos of the 3-D wake. All results from *Re*=∞ simulations.

At the beginning of Stage 1, a tube-like vortical structure develops at the fins and tail (see Fig. 5A). This vortical structure consists of vortex tubes created by the fins (denoted by F1 in Fig. 5A) and the tail (denoted by T1 in Fig. 5A), which at this instant are connected together to form a single, continuous starting vortex loop for the sunfish with all fins. The sunfish with anal/dorsal fins removed/erected (Fig. 5A, middle) forms a T1 similar to the sunfish with all fins. However, their S-shaped F1 structure is straighter than and not as round as the sunfish with all fins. The sunfish with no tail (Fig. 5A, right) does not form the T1 structure like the others, but the F1 structure is similar to the sunfish with all fins.

During Stage 1, as the sunfish bends its body into the C-shape (Fig. 5B), the T1 and F1 vortex tubes are seen to deform along with the moving body. The T1 vortex loop in the three sunfish with tails is quite similar and does not exist in the sunfish with no tail, i.e. the T1 vortex is the largest difference between the wakes of the three sunfish. The F1 vortex with an S-shape is quite similar in the sunfish with no tail and the sunfish with all fins. However, the F1 vortices in the sunfish with anal/dorsal fins removed/erected are slightly different and not as round as the control sunfish because the removal/erection of the anal/dorsal fins has created a straighter edge than the control sunfish. Another vortex loop F2 is also created at this time due to the motion of body whose sense of rotation is opposite to that of the starting F1 loop. The shape of this loop (F2) in the sunfish with anal/dorsal fins removed/erected is also not as round as the control sunfish is straight.

During Stage 2, as the sunfish is moving out of the C-bend, the T1 and T2 structures created by the tail are visible in the sunfish with a tail (Fig. 5C). These structures are not present in the wake of the sunfish with no tail (Fig. 5C). Instead, the fin-created

structures (F1 to F4) are present in both sides of the tail-less sunfish, which are connected by an almost straight vortex tube created by the straight edge at the end of the body where the tail has been cut off. The vortex tubes F1 to F4 in the sunfish with no tail are quite similar to the sunfish with all fins. These structures are also present in the sunfish with anal/dorsal fins removed/erected (Fig. 5C), but their shape is somewhat different (straighter) due to the straight shape of the edge that forms them instead of the smaller edge in the control anal/dorsal fins. Nevertheless, the difference in the wake structure due to the removal of the anal/dorsal fins is less conspicuous than the removal of the tail at this instant. This is also true at later instants (Fig. 5D), e.g. end of Stage 2 at t=71 ms in which the wake structure for the two sunfish with the tail consists of multiple vortex loops, whereas the wake of the tail-less sunfish does not have similar vortex loops. The tail-less sunfish wake mainly consists of anal/dorsal fin structures that are connected with a straight tube vortex, created by the straight edge where the tail was removed, and has become unstable at this instant (Fig. 5D).

DISCUSSION

Investigating the role of fins during the C-start experimentally is quite challenging mainly due to issues with controlling live fish, i.e. there are no guarantees that live fish with different fins perform a C-start maneuver exactly the same. Measuring the force produced by individual fins is also quite challenging, both experimentally and numerically. Experimentally guided numerical simulations have allowed investigation of the effect of fins on the C-start by comparing four different swimmers under exactly the same conditions. Comparing different swimmers under similar conditions is quite difficult experimentally since two swimmers rarely perform C-starts similarly. Therefore, many C-start trials are needed in experiments to reach statistical results, which are not sensitive to the number of trials, e.g. see Webb's experimental study (Webb, 1977) on C-start. In the numerical simulations here, different swimmers perform exactly the same C-start maneuver under similar flow conditions. Therefore, statistical analysis was not required in this study since different swimmers can be compared using only one C-start maneuver. The instantaneous hydrodynamic force and flow field created by the different virtual sunfish were compared in the previous section. In what follows, the flow field and forces obtained in this work are compared and contrasted against previous investigations to discuss how these results affect and influence the current knowledge of how fins work during C-start maneuvers.

The relation of wake structure and hydrodynamic force

This study builds upon the previous work of Borazjani et al. (Borazjani et al., 2012), in which the numerical method was validated against the experimental flow measurement of Tytell and Lauder (Tytell and Lauder, 2008) for a sunfish whose kinematics was prescribed in the simulations. The simulations of the sunfish with all fins could capture all the flow features including the triple jet flows observed experimentally (Tytell and Lauder, 2008). The vorticity in the wake structure agrees well with previously observed wakes in experimental work on turning maneuvers (Wolfgang et al., 1999; Epps and Techet, 2007; Müller et al., 2008). In fact, vortices VT1, VT2 and VT3 are all visible in the PIV measurements of Epps and Techet (Epps and Techet, 2007), although the turning of giant danio (~200 ms) is much slower than the sunfish maneuver here (~60 ms).

The experimental measurements of the wake have provided the flow field in one or several 2-D planes in flow (Wolfgang et al., 1999; Epps and Techet, 2007; Müller et al., 2008; Tytell and Lauder, 2008). Nevertheless, the 3-D flow field, which is essential for estimating hydrodynamic forces, can be obtained by the experimentally guided simulation. Borazjani et al. (Borazjani et al., 2012) elucidated the 3-D wake structure during the C-start of sunfish for the first time. They showed the relation of the 3-D wake with the vorticity observed in the 2-D planes from experimental measurements, which are the footprints of the 3-D structures (Borazjani et al., 2012). Knowledge of the correct 3-D structure is essential for estimating momentum and hydrodynamic forces from the measured 2-D flow field because the measurements in a plane can only provide forces per unit height in that plane (Tytell, 2007). Estimating the height usually involves some assumptions regarding the 3-D structure of the wake, e.g. vortex ring, or building an empirical relation for momentum per height from center to tip of the fins (Tytell, 2007). Furthermore, a pressure-like term is also required for estimating forces from flow measurements (Dabiri, 2005). Here the hydrodynamic forces are calculated based on the 3-D pressure and flow field created by the motion of the sunfish.

The wake structure and hydrodynamic force are closely related. The rate of momentum change in the wake equals the force exerted by fish to the water. According to Newton's third law of motion, the reaction to this force (equal but opposite direction) is the hydrodynamic force exerted by the water to the fish's center of mass. The increase in the momentum of Jet 2 will generate the hydrodynamic force to accelerate the fish in the positive x-direction away from the stimulus (Tytell and Lauder, 2008). Jet 2 flows through the 3-D wake structures T2 to T4, which are mainly created by the tail (Fig. 5). The removal of the tail drastically affects the 3-D wake structure. As can be observed in Fig. 5, the removal of the tail eliminates the vortex loop T1 and the corresponding experimentally observed Jet 1 flows (Tytell and Lauder, 2008) through it (Fig. 4). Moreover, it eliminates the vortex loops T2 to T4 (Fig. 5), which add momentum to Jet 2 (Fig. 4). The removal of the anal/dorsal fins affects the shape of the fin-generated wake, which is smaller and less prominent than the wake created by the tail (Fig. 5). This is consistent with the force history in showing relatively smaller changes in the total hydrodynamic force by the removal/erection of the anal/dorsal fins relative to the caudal fin (Fig. 3).

The author is not aware of any work investigating the wake of fish with any fins amputated; therefore, no direct comparison is possible. However, previous work on comparing the simulated and experimentally measured wake (Borazjani et al., 2012) builds confidence in the results presented here. The 3-D wake structure is also quite important in predator–prey interaction, which makes the fish conspicuous to predators. It is observed that the erection of the fins does not drastically change the wake structure (Fig. 5). In fact, the wake structure of the control sunfish and the sunfish with fins erected can both be fitted in a cube of size $L\times0.5L\times L$, surrounding the fish in the x-, y- and z-directions, respectively. The wake flow patterns produced by steady swimming or low-frequency flapping are known to be used by predators to track prey (Dehnhardt et al., 2001; Hanke and Bleckmann, 2004; Wieskotten et al., 2010). Based on the 3-D wake presented here (Fig. 5), it can be concluded that the erection of the fins does not affect such tracking, if possible, by predators.

The role of fins during the C-start

The current consensus on the role of fins (both caudal and anal/dorsal fins) during the C-start is that they are used to create a large hydrodynamic force for rapid acceleration of the sunfish. As a result, the erection of the anal/dorsal fins during the C-start (Webb, 1977;

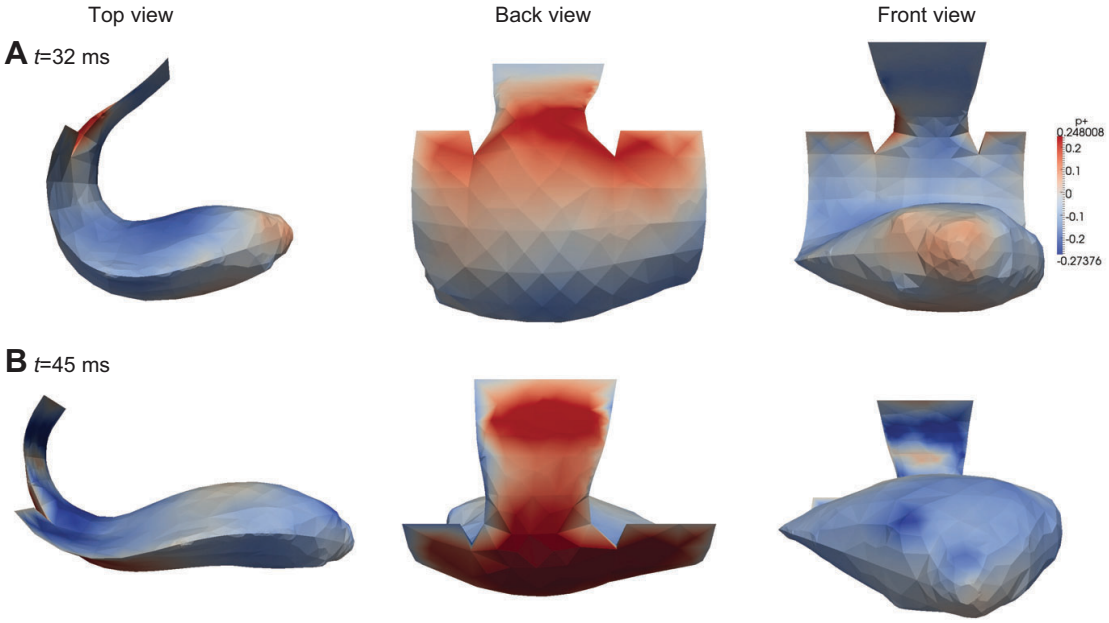

Fig. 6. The non-dimensional pressure (p+) on the fish body from different views just before Stage 2 (top row, t=32 ms) and in the middle of Stage 2 (bottom row, t=45 ms).

Tytell and Lauder, 2002) has been attributed to generating hydrodynamic force. The results presented here support this view for the caudal fin, but not necessarily for the anal/dorsal fins. The role of anal/dorsal fin erection for stability of the fish during the C-start, in my opinion, has not been fully explored. In what follows, a summary of previous work supporting the consensus is presented and compared/contrasted with the results presented here. Finally, the role of anal/dorsal fins for the stability of the sunfish during the C-start is discussed based on conservation of angular momentum.

According to the EBT model of Weihs, the caudal fin generates the majority of hydrodynamic force during the C-start because the highest acceleration occurs in that region, i.e. high added mass force (Weihs, 1973). Webb (Webb, 1977) studied the effect of different fins on live fish by amputating different groups of fins as discussed earlier in the Introduction. The reduction in C-start performance caused by the removal of the caudal fin was statistically significant (more than 5%). However, the reduction in C-start performance caused by the removal of dorsal/anal fins was not statistically significant (less than 5%). Therefore, no definitive conclusions on the effect of dorsal and anal fin removal could be made due to the statistically insignificant differences (Webb, 1977), despite the theory predicting that the increase in size (area) of the fish (by fins) should increase the C-start performance (Weihs, 1973).

Webb's findings (Webb, 1977) are in agreement with the present results, showing that the removal/erection of the anal/dorsal fins did not affect the forces during the C-start, whereas the removal of the caudal fin caused considerable changes in the force history (Fig. 3). In fact, it can be observed that during the C-start the difference between the hydrodynamic force created by the control sunfish and the sunfish with anal/dorsal fins removed or erected is less than 5% at each time instant, except for a short time at the end of Stage 1 (t ~30 ms). During the short period of force burst just before Stage 2 (t=30 to 32 ms), about 70% of the force in the x-direction is generated by the tail, about 19% by the erected fins, and the rest by the body. The fin erection has increased the force in the x-direction by about 17% (relative to the control sunfish) in this short period before Stage 2 (Fig. 3). This amount of increase in the force just before Stage 2 can help accelerate the sunfish in the escape (x) direction during Stage 2 when the sunfish bends out of the C-shape. To identify why the fin erection has a higher contribution during this short period relative to the other time instants during the cycle, the pressure (non-dimensionalized by ρU^2) on the fish body is visualized at the beginning of Stage 2 (t=32 ms) and the middle of Stage 2 (t=45 ms) in Fig. 6. It can be observed that at the beginning of Stage 1 (Fig. 6A) the highest pressure occurs at the base of the tail and fins on the pressure side (back view), while the lowest pressure occurs on the suction side (front view). At this instant (t=32 ms), the anal/dorsal fins and the base of the tail are almost perpendicular to the x-direction, which combined with high pressure difference between the sides of the fins creates considerable force in the x-direction (Fig. 6A). In the middle of Stage 2, in contrast, the high pressure region is almost at the end of the tail while the tail is mainly perpendicular to the x-direction and the body and fins are almost parallel to the x-direction (Fig. 6B). This enables the tail (not the anal/dorsal fins) to generate most of the force in the x-direction during Stage 2 (Fig. 6B).

Frith and Blake (Frith and Blake, 1991) used Weihs's EBT model to calculate the hydrodynamic force generated during the C-start of northern pike, *Esox lucius*. They divided the pike body into nine sections and calculated the added mass and lift force created by each section. Their calculated force history (e.g. see fig. 10B of their paper) is quite similar to the force history observed here (Fig. 3), and shows large-amplitude fluctuations (positive and negative extrema) over a time scale of the order of a few milliseconds. Based on their calculations, about 77% of positive total thrust was generated by the tail during Stage 2 of the C-start (Frith and Blake, 1991). Nevertheless, the amount of force produced by the caudal fin was not constant and varied during the C-start; see fig. 10B of their paper (Frith and Blake, 1991). This is in agreement with our results showing that the effect of caudal fin removal is not similar throughout the C-start maneuver and is maximized at the end of Stage 1 and beginning of Stage 2 (Fig. 3). In fact, at the beginning of Stage 2, more than 70% of the total force in the x-direction is generated by the caudal fin, whereas in Stage 1, only about 20% of

the force in the *x*-direction is generated by the caudal fin (Fig. 3). This is in agreement with their calculations that 77% of the total positive thrust is created by the tail (Frith and Blake, 1991), which shows the importance of the tail in generating hydrodynamic force for rapid acceleration of the sunfish during the C-start.

The generation of a large force by the tail during Stage 2 can be explained by the fact that the high acceleration and large area of the tail normal to the direction of motion creates high added mass (reactive) forces (Weihs, 1972; Weihs, 1973). The added mass forces are generated earlier than the lift forces in Stage 2 (Frith and Blake, 1991), and can be considered as the main source of the large hydrodynamic force observed in late Stage 1 and early Stage 2 in Fig. 3. During Stage 2, the sunfish moves the caudal fin such that it remains perpendicular to the direction of motion (mainly *x*-direction; see supplementary material Movies 1–3 of the C-start, or the inset of Fig. 3C), i.e. maintains a large area perpendicular to the direction of motion that adds momentum to Jet 2 (Fig. 4C). Large amounts of added mass force are created early in Stage 2 (Fig. 3) due to maintaining a large area together with the high acceleration of the caudal fin in Stage 2, when the fish bends out of the C-shape.

Based on the results presented here and in previous work (Weihs, 1972; Weihs, 1973; Webb, 1977; Webb, 1978; Frith and Blake, 1991; Tytell and Lauder, 2008), it is reasonable to argue that the function of the caudal fin during the C-start is to generate high hydrodynamic forces during Stage 2 of the C-start, which rapidly accelerates the sunfish. The role of anal and caudal fins, however, is more controversial. The results of Webb (Webb, 1977) for amputation of anal/dorsal fin was not statistically significant and showed less than a 5% reduction in performance. However, Frith and Blake (Frith and Blake, 1991) estimated that ~28% of the total positive thrust is produced by the anal and dorsal fins. Tytell and Lauder also estimated that 37% of the total momentum is contributed by anal and dorsal fins (Tytell and Lauder, 2008). Finally, the results presented here suggest that during most of the C-start, except for a period of a few milliseconds before the beginning of Stage 2, the forces created by the anal/dorsal fins account for less than 5% of the hydrodynamic force at each instant.

To reconcile these apparently contradicting studies, one needs to look at these studies more closely. By examining the results of Frith and Blake, it can be observed that the body in between the anal and dorsal fins is also included in calculations for the reported 28% positive thrust [see section 3 definition in fig. 1A of their paper (Frith and Blake, 1991)], i.e. the reported 28% positive thrust includes contributions from the body in between the fins. Tytell and Lauder report that 37% of total momentum is generated by the anal and dorsal fins by calculating the momentum of the wake on a horizontal plane passing through the anal and dorsal fins (Tytell and Lauder, 2008). However, the planes also cut through some parts of the body; see fig. 6 of their paper (Tytell and Lauder, 2008). They cautioned that those parts of the body can add to the momentum of the wake as well (Tytell and Lauder, 2008). Moreover, they state that most of the momentum produced by the anal and dorsal fins occurs during Stage 1, i.e. 28% of the total momentum by the end of Stage 1 and 37% by the end of Stage 2 is generated by the anal and dorsal fins by adding momentum to Jet 2 (Tytell and Lauder, 2008). The results presented here also show that most of the hydrodynamic force produced is not by the tail (Fig. 3) because the effect of the tail on the hydrodynamic force during Stage 1 is less than 20%. The results presented here indicate that most of the hydrodynamic force in Stage 1 is produced by the deep body of the sunfish and not the anal and dorsal fins. This can be observed in Fig. 3, which shows that the removal and erection of anal and dorsal fins did not change the hydrodynamic force produced except for a short period at the end of Stage 1. Finally, it should be noted that the EBT method of Weihs (Weihs, 1972; Weihs, 1973) applied to the sunfish might confirm this finding. This is due to the fact that according to the theory the deepest section releases a wake of the same depth, thus making the section depth reductions posterior to the deepest section irrelevant to the added mass forces. Sunfish, as opposed to trout, pike, etc., have their deepest section anterior to the dorsal/anal fins (Fig. 1), i.e. based on the theory (Weihs, 1972; Weihs, 1973) that the anal/dorsal fin erection in the sunfish does not contribute to the added mass force. However, it will affect the lift forces generated by these fins (Weihs, 1972; Weihs, 1973).

The above discussion leads to the conclusion that the major role of anal and dorsal fins during the C-start might not be to produce hydrodynamic force except for a short period just before Stage 2. This is quite surprising since the anal and dorsal fins are rapidly erected to increase their surface area during the C-start (Webb, 1977; Jayne et al., 1996; Tytell and Lauder, 2008). Furthermore, muscle activity measurements have shown that the anal and dorsal fins are controlled actively by the muscles during the C-start and not just for a short period (Jayne et al., 1996; Standen and Lauder, 2005; Lauder et al., 2007; Chadwell and Ashley-Ross, 2012; Chadwell et al., 2012b; Chadwell et al., 2012a). Therefore, we hypothesize that the anal and dorsal fins have a more significant role in preserving the stability of the fish during the C-start than in producing the hydrodynamic force to accelerate the sunfish. It is hypothesized here that the active control and erection of fins during the C-start is related to maintaining the stability of the fish against roll and pitch movements. This issue will be discussed in more detail in the next section.

The role of anal/dorsal fin erection on stability during the C-start

Stability is the ability of the system to self-correct for disturbances and maintain a desired postural attitude, whereas maneuvering is the ability of the system to do the opposite by producing controlled instabilities allowing a change in direction, stopping and starting (Fish, 2002; Weihs, 2002; Webb, 2005). This definition readily indicates a conflict between stability and maneuverability (Fish, 2002; Weihs, 2002; Webb, 2005). Stability is traditionally considered as promoting steady movement along a trajectory, but maneuverability is changing the trajectory as desired (Fish, 2002).

During the C-start, the fish remains mostly in a horizontal plane while changing its orientations. The change in the orientation usually involves a yawing motion but not rolling or pitching motion (see Fig. 7 for the definition of roll, pitch and yaw). Therefore, the fish is required to be maneuverable for the yawing motion but stable with respect to pitching and rolling motions.

The cross-sections promoting stability are more circular, whereas the cross-sections promoting maneuverability are deeper (Webb, 1978; Fish, 2002; Weihs, 2002). Based on such traditional definitions, the erection of the anal and dorsal fins will make the fish more maneuverable but less stable. However, it is argued here that the erection of the anal and dorsal fins makes the fish more maneuverable for the yawing motion and more stable for the pitching and rolling motions. The erection of the anal and dorsal fins increases the moment of inertia defined as:

$$I_{ii} = \int r_i^2 \, dm, \quad (2)$$

where I_{ii} is the moment of inertia around axis ii, dm is the mass differential, and r_i is the distance of the mass differential from the axis ii, and the integral is over the volume of the body. Note that

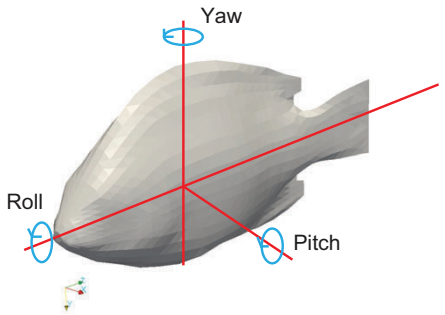

Fig. 7. The roll, pitch and yaw angles for a fish. During the C-start, the sunfish rotates around the yaw axis but not around the roll or pitch axes. The erection of the fins increases the moment of inertia around the roll and pitch axes, but not around the yaw axis.

the erection of the fins increases the moment of inertia around the pitch and roll axes, but not the yaw axis because the erection is parallel to the yaw axis and does not increase r_i from that axis. The increase in the moment of inertia requires higher pitching and rolling moments to rotate the fish around roll and pitch axes, i.e. making the rolling and pitching movements more difficult.

Due to dorsoventral asymmetry of the fish, rolling and pitching moments are produced. The only way to overcome such moments is by active control of the fins, especially the anal and dorsal fins. This is in agreement with previous muscle activity measurements showing active control of the anal and dorsal fins during the C-start (Jayne and Lauder, 1993; Tytell and Lauder, 2002). Similar active control of the dorsal fin has also been observed in steady swimming of sharks (Lingham□Soliar, 2005). During fast swimming the dorsal fins are stiffened, while during slow swimming the fibers are slackened and the fin becomes more flexible (Lingham□Soliar, 2005).

Recent work of Chadwell et al. (Chadwell et al., 2012a; Chadwell et al., 2012b) on anal and dorsal fin kinematics during the C-start of a bluegill sunfish also shows that the fin-ray kinematics vary with position and do not act as uniform structures. Furthermore, the kinematic patterns observed there supported the predictions that the anal and dorsal fins are actively resisting hydrodynamic forces and transmitting momentum into the water (Chadwell et al., 2012a; Chadwell et al., 2012b). As shown here, the magnitude of the hydrodynamic force produced by these fins during the C-start is not large relative to the body or the caudal fin. However, because the distance of these fins to the roll and pitch axes is large (moment = distance × force), they can contribute and balance the rolling and pitching moments during the C-start. Such balance of pitching and rolling moments is critical if the fish wants to stay in the same plane during the C-start. The effects of the fins on the stability will be investigated in future by prescribing the detailed motion of the fins while calculating the rotation of sunfish with respect to the roll, pitch and yaw axes through a fluid–structure interaction algorithm.

ACKNOWLEDGEMENTS

The author thanks Haridas Attur and Varunkumar Vruddhula for creating different sunfish geometries used in this work. The author is grateful to Fotis Sotiropoulos, George Lauder and Eric Tytell for their helpful discussions and support.

COMPETING INTERESTS

No competing interests declared.

FUNDING

This work was partly supported by the Center for Computational Research (CCR) at the University at Buffalo.

REFERENCES

Balay, S., Buschelman, K. Gropp, W. D., Kaushik, D., Knepley, M. G., McInnes, L. C., Smith, B. F. and Zhang, H. (2001). PETSc Web page http://www.mcs.anl.gov/petsc/.

Bergstrom, C. (2002). Fast-start swimming performance and reduction in lateral plate number in threespine stickleback. *Can. J. Zool.* **80**, 207-213.

Blake, R. (2004). Fish functional design and swimming performance. *J. Fish Biol.* **65**, 1193-1222.

Borazjani, I. and Sotiropoulos, F. (2008). Numerical investigation of the hydrodynamics of carangiform swimming in the transitional and inertial flow regimes. *J. Exp. Biol.* **211**, 1541-1558.

Borazjani, I. and Sotiropoulos, F. (2009). Numerical investigation of the hydrodynamics of anguilliform swimming in the transitional and inertial flow regimes. *J. Exp. Biol.* **212**, 576-592.

Borazjani, I. and Sotiropoulos, F. (2010). On the role of form and kinematics on the hydrodynamics of self-propelled body/caudal fin swimming. *J. Exp. Biol.* **213**, 89-107.

Borazjani, I., Ge, L. and Sotiropoulos, F. (2008). Curvilinear immersed boundary method for simulating fluid structure interaction with complex 3D rigid bodies. *J. Comput. Phys.* **227**, 7587-7620.

Borazjani, I., Sotiropoulos, F., Malkiel, E. and Katz, J. (2010). On the role of copepod antennae in the production of hydrodynamic force during hopping. *J. Exp. Biol.* **213**, 3019-3035.

Borazjani, I., Sotiropoulos, F., Tytell, E. D. and Lauder, G. V. (2012). Hydrodynamics of the bluegill sunfish C-start escape response: three-dimensional simulations and comparison with experimental data. *J. Exp. Biol.* **215**, 671-684.

Canfield, J. G. and Rose, G. J. (1993). Activation of Mauthner neurons during prey capture. *J. Comp. Physiol. A* **172**, 611-618.

Chadwell, B. A. and Ashley-Ross, M. A. (2012). Musculoskeletal morphology and regionalization within the dorsal and anal fins of bluegill sunfish (*Lepomis macrochirus*). *J. Morphol.* **273**, 405-422.

Chadwell, B. A., Standen, E. M., Lauder, G. V. and Ashley-Ross, M. A. (2012a). Median fin function during the escape response of bluegill sunfish (*Lepomis macrochirus*). I: Fin-ray orientation and movement. *J. Exp. Biol.* **215**, 2869-2880.

Chadwell, B. A., Standen, E. M., Lauder, G. V. and Ashley-Ross, M. A. (2012b). Median fin function during the escape response of bluegill sunfish (*Lepomis macrochirus*). II: Fin-ray curvature. *J. Exp. Biol.* **215**, 2881-2890.

Conte, J., Modarres-Sadeghi, Y., Watts, M. N., Hover, F. S. and Triantafyllou, M. S. (2010). A fast-starting mechanical fish that accelerates at 40 m s^{-2}. *Bioinspir. Biomim.* **5**, 035004.

Dabiri, J. O. (2005). On the estimation of swimming and flying forces from wake measurements. *J. Exp. Biol.* **208**, 3519-3532.

Dehnhardt, G., Mauck, B., Hanke, W. and Bleckmann, H. (2001). Hydrodynamic trail-following in harbor seals (*Phoca vitulina*). *Science* **293**, 102-104.

DeVoria, A. C. and Ringuette, M. J. (2012). Vortex formation and saturation for low-aspect-ratio rotating flat-plate fins. *Exp. Fluids* **52**, 441-462.

Domenici, P. and Batty, R. S. (1997). Escape behaviour of solitary herring (*Clupea harengus*) and comparisons with schooling individuals. *Mar. Biol.* **128**, 29-38.

Domenici, P. and Blake, R. W. (1991). The kinematics and performance of the escape response in the angelfish (*Pterophyllum eimekei*). *J. Exp. Biol.* **156**, 187-205.

Domenici, P. and Blake, R. W. (1993). Escape trajectories in angelfish (*Pterophyllum eimekei*). *J. Exp. Biol.* **177**, 253-272.

Domenici, P. and Blake, R. (1997). The kinematics and performance of fish fast-start swimming. *J. Exp. Biol.* **200**, 1165-1178.

Domenici, P., Standen, E. M. and Levine, R. P. (2004). Escape manoeuvres in the spiny dogfish (*Squalus acanthias*). *J. Exp. Biol.* **207**, 2339-2349.

Eaton, R. C., Lee, R. K. K. and Foreman, M. B. (2001). The Mauthner cell and other identified neurons of the brainstem escape network of fish. *Prog. Neurobiol.* **63**, 467-485.

Ellerby, D. J. and Altringham, J. D. (2001). Spatial variation in fast muscle function of the rainbow trout *Oncorhynchus mykiss* during fast-starts and sprinting. *J. Exp. Biol.* **204**, 2239-2250.

Epps, B. P. and Techet, A. H. (2007). Impulse generated during unsteady maneuvering of swimming fish. *Exp. Fluids* **43**, 691-700.

Fetcho, J. R. (1991). Spinal network of the Mauthner cell. *Brain Behav. Evol.* **37**, 298-316.

Fish, F. E. (2002). Balancing requirements for stability and maneuverability in cetaceans. *Integr. Comp. Biol.* **42**, 85-93.

Frith, H. and Blake, R. (1991). Mechanics of the startle response in the northern pike, *Esox lucius*. *Can. J. Zool.* **69**, 2831-2839.

Gazzola, M., Van Rees, W. M. and Koumoutsakos, P. (2012). C-start: optimal start of larval fish. *J. Fluid Mech.* **698**, 5-18.

Ge, L. and Sotiropoulos, F. (2007). A numerical method for solving the 3D unsteady incompressible Navier-Stokes equations in curvilinear domains with complex immersed boundaries. *J. Comput. Phys.* **225**, 1782-1809.

Gilmanov, A. and Sotiropoulos, F. (2005). A hybrid Cartesian/immersed boundary method for simulating flows with 3D, geometrically complex, moving bodies. *J. Comput. Phys.* **207**, 457-492.

Hanke, W. and Bleckmann, H. (2004). The hydrodynamic trails of *Lepomis gibbosus* (Centrarchidae), *Colomesus psittacus* (Tetraodontidae) and *Thysochromis ansorgii* (Cichlidae) investigated with scanning particle image velocimetry. *J. Exp. Biol.* **207**, 1585-1596.

Harper, D. G. and Blake, R. W. (1988). Energetics of piscivorous predator-prey interactions. *J. Theor. Biol.* **134**, 59-76.

Harper, D. G. and Blake, R. W. (1989). On the error involved in high-speed film when used to evaluate maximum accelerations of fish. *Can. J. Zool.* **67**, 1929-1936.

Harper, D. G. and Blake, R. W. (1991). Prey capture and the fast-start performance of northern pike *Esox lucius*. *J. Exp. Biol.* **155**, 175-192.

Hunt, J. C. R., Wray, A. A. and Moin, P. (1988). Eddies, streams, and convergence zones in turbulent flows. In *Studying Turbulence Using Numerical Simulation*

Databases, 2. Proceedings of the 1988 Summer Program (NASA Contractor Report) pp. 193-208. Stanford, CA: Ames Research Center/Center for Turbulence Research.
Jacobs, P. A. and Lott, N. J. (1989). CMATH – A Mathematical Software Library for the C Programming Language. Queensland, Australia: Design Software.
Jayne, B. C. and Lauder, G. V. (1993). Red and white muscle activity and kinematics of the escape response of the bluegill sunfish during swimming. *J. Comp. Physiol. A* **173**, 495-508.
Jayne, B. C., Lozada, A. F. and Lauder, G. V. (1996). Function of the dorsal fin in bluegill sunfish: motor patterns during four distinct locomotor behaviors. *J. Morphol.* **228**, 307-326.
Koyama, M., Kinkhabwala, A., Satou, C., Higashijima, S.-i. and Fetcho, J. (2011). Mapping a sensory-motor network onto a structural and functional ground plan in the hindbrain. *Proc. Natl. Acad. Sci. USA* **108**, 1170-1175.
Lauder, G. V., Anderson, E. J., Tangorra, J. and Madden, P. G. A. (2007). Fish biorobotics: kinematics and hydrodynamics of self-propulsion. *J. Exp. Biol.* **210**, 2767-2780.
Lighthill, M. J. (1971). Large-amplitude elongated-body theory of fish locomotion. *Proc. R. Soc. B* **179**, 125-138.
Lingham-Soliar, T. (2005). Dorsal fin in the white shark, *Carcharodon carcharias*: a dynamic stabilizer for fast swimming. *J. Morphol.* **263**, 1-11.
Müller, U. K., van den Boogaart, J. G. M. and van Leeuwen, J. L. (2008). Flow patterns of larval fish: undulatory swimming in the intermediate flow regime. *J. Exp. Biol.* **211**, 196-205.
Saad, Y. (2003). *Iterative Methods for Sparse Linear Systems*. Philadelphia, PA: SIAM.
Spierts, I. L. and Leeuwen, J. L. (1999). Kinematics and muscle dynamics of C- and S-starts of carp (*Cyprinus carpio* L.). *J. Exp. Biol.* **202**, 393-406.
Standen, E. M. and Lauder, G. V. (2005). Dorsal and anal fin function in bluegill sunfish *Lepomis macrochirus*: three-dimensional kinematics during propulsion and maneuvering. *J. Exp. Biol.* **208**, 2753-2763.
Tytell, E. (2007). Do trout swim better than eels? Challenges for estimating performance based on the wake of self-propelled bodies. *Exp. Fluids* **43**, 701-712.
Tytell, E. D. and Lauder, G. V. (2002). The C-start escape response of *Polypterus senegalus*: bilateral muscle activity and variation during Stage 1 and 2. *J. Exp. Biol.* **205**, 2591-2603.
Tytell, E. D. and Lauder, G. V. (2008). Hydrodynamics of the escape response in bluegill sunfish, *Lepomis macrochirus*. *J. Exp. Biol.* **211**, 3359-3369.
Wakeling, J. M. and Johnston, I. A. (1998). Muscle power output limits fast-start performance in fish. *J. Exp. Biol.* **201**, 1505-1526.
Wakeling, J. M. and Johnston, I. A. (1999). Predicting muscle force generation during fast-starts for the common carp *Cyprinus carpio*. *J. Comp. Physiol. B* **169**, 391-401.
Wakeling, J. M., Kemp, K. M. and Johnston, I. A. (1999). The biomechanics of fast-starts during ontogeny in the common carp *Cyprinus carpio*. *J. Exp. Biol.* **202**, 3057-3067.
Walker, J. A. (1998). Estimating velocities and accelerations of animal locomotion: a simulation experiment comparing numerical differentiation algorithms. *J. Exp. Biol.* **201**, 981-995.
Walker, J. A., Ghalambor, C. K., Griset, O. L., McKenney, D. and Reznick, D. N. (2005). Do faster starts increase the probability of evading predators? *Funct. Ecol.* **19**, 808-815.
Webb, P. (1977). Effects of median-fin amputation on fast-start performance of rainbow trout (*Salmo gairdneri*). *J. Exp. Biol.* **68**, 123-125.
Webb, P. W. (1978). Fast-start performance and body form in seven species of teleost fish. *J. Exp. Biol.* **74**, 211-226.
Webb, P. W. (1984). Body and fin form and strike tactics of four teleost predators attacking fathead minnow (*Pimephales promelas*) prey. *Can. J. Fish. Aquat. Sci.* **41**, 157-165.
Webb, P. W. (2005). Stability and maneuverability. *Fish Physiol.* **23**, 281-332.
Webb, P. W. and Skadsen, J. M. (1980). Strike tactics of *Esox*. *Can. J. Zool.* **58**, 1462-1469.
Webb, P. W., LaLiberte, G. D. and Schrank, A. J. (1996). Does body and fin form affect the maneuverability of fish traversing vertical and horizontal slits? *Environ. Biol. Fish* **46**, 7-14.
Weihs, D. (1972). A hydrodynamical analysis of fish turning manoeuvres. *Proc. R. Soc. B* **182**, 59-72.
Weihs, D. (1973). The mechanism of rapid starting of slender fish. *Biorheology* **10**, 343-350.
Weihs, D. (2002). Stability versus maneuverability in aquatic locomotion. *Integr. Comp. Biol.* **42**, 127-134.
Westneat, M. W., Hale, M. E., Mchenry, M. J. and Long, J. H. (1998). Mechanics of the fast-start: muscle function and the role of intramuscular pressure in the escape behavior of *Amia calva* and *Polypterus palmas*. *J. Exp. Biol.* **201**, 3041-3055.
Wieskotten, S., Dehnhardt, G., Mauck, B., Miersch, L. and Hanke, W. (2010). Hydrodynamic determination of the moving direction of an artificial fin by a harbour seal (*Phoca vitulina*). *J. Exp. Biol.* **213**, 2194-2200.
Wolfgang, M. J., Anderson, J. M., Grosenbaugh, M. A., Yue, D. K. and Triantafyllou, M. S. (1999). Near-body flow dynamics in swimming fish. *J. Exp. Biol.* **202**, 2303-2327.
Zottoli, S. J., Bentley, A. P., Prendergast, B. J. and Rieff, H. I. (1995). Comparative studies on the Mauthner cell of teleost fish in relation to sensory input. *Brain Behav. Evol.* **46**, 151-164.